

The Poisson tensor completion non-parametric differential entropy estimator

Daniel M. Dunlavy*, Richard B. Lehoucq†, Carolyn D. Mayer‡, and Arvind Prasad‡
Sandia National Laboratories, Albuquerque, NM and Livermore, CA

Abstract

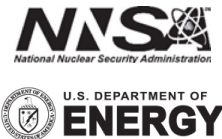
We introduce the *Poisson tensor completion (PTC) estimator*, a non-parametric differential entropy estimator. The PTC estimator leverages inter-sample relationships to compute a low-rank Poisson tensor decomposition of the frequency histogram. Our crucial observation is that the histogram bins are an instance of a space partitioning of counts and thus can be identified with a spatial Poisson process. The Poisson tensor decomposition leads to a completion of the intensity measure over all bins—including those containing few to no samples—and leads to our proposed PTC differential entropy estimator. A Poisson tensor decomposition models the underlying distribution of the count data and guarantees non-negative estimated values and so can be safely used directly in entropy estimation. Our estimator is the first tensor-based estimator that exploits the underlying spatial Poisson process related to the histogram explicitly when estimating the probability density with low-rank tensor decompositions for the purpose of tensor completion. Furthermore, we demonstrate that our PTC estimator is a substantial improvement over standard histogram-based estimators for sub-Gaussian probability distributions because of the concentration of norm phenomenon.

1 Introduction

The differential entropy of a multivariate random variable has practical use in a number of applications in addition to the intrinsic mathematical and statistical desire to estimate entropy from sample observations. Example applications in statistical modeling include goodness-of-fit tests and tests of uniformity [1, 2], alternatives to maximum likelihood estimators in settings where such estimators are not consistent [3], feature selection in biostatistics and machine learning models with tens of thousands of features [4], and independent component analysis applied to blind source separation problems [5, 6]. In addition, differential entropy has been used in quantifying the thermodynamics [7] of a computational process.

A recent result [8] explains that histogram-based estimators for the differential entropy of a multivariate random variable are asymptotically optimal. Unfortunately, in practice, we are often limited to a finite sample of the unknown probability density upon which the differential entropy relies. It is also well understood that the accuracy of histogram-based probability density estimators depends upon an exponentially large number of bins as the number of variates (see, e.g., [9]) increases. This suggests that the histogram data can be better leveraged by exploiting inherent relational structure across the samples and/or bins. In previous work, Vandermeulen and Ledent demonstrate that leveraging low-rank models of the histogram counts can lead to improved estimates of the density over histogram-based estimators using the same samples and bins [10]. However, their approach assumes near independence of the variates and does not explicitly account for the underlying distribution of the histogram data, thus providing opportunities for estimator improvements and applicability to more general multivariate distributions.

*dmdunla@sandia.gov, †rblehou@sandia.gov, ‡cdmayer@sandia.gov, §aprasad@sandia.gov



Sandia National Laboratories is a multimission laboratory managed and operated by National Technology & Engineering Solutions of Sandia, LLC, a wholly owned subsidiary of Honeywell International Inc., for the U.S. Department of Energy's National Nuclear Security Administration under contract DE-NA0003525. SAND2025-05664R

Our contribution is the non-parametric *Poisson tensor completion (PTC)* differential entropy estimator that expands on this previous work, explicitly modeling the underlying distribution of the histogram data by exploiting relationship between frequency histograms, spatial Poisson processes, and low-rank Poisson tensor decompositions. The PTC estimator leverages inter-sample relationships by computing a low-rank decomposition of the frequency histogram, which is an instance of a tensor, or multi-dimensional array. However, we observe that the histogram bins are an instance of a space partitioning of counts and thus can be identified with a spatial Poisson process—enabling us to remove the assumption made by Vandermeulen and Ledent that the variates are nearly independent. Following this observation, we compute a low-rank Poisson tensor decomposition [11] of the histogram bin counts to approximate the Poisson intensity measure, which is the probability density integrated over the bins. A Poisson tensor decomposition models the underlying distribution of the count data and guarantees non-negative estimated values and so can safely be used directly in entropy estimation. The Poisson tensor decomposition leads to a completion of the intensity measure over all bins—including those containing a few to no samples—and leads to our proposed PTC differential entropy estimator. We believe our estimator is the first tensor-based estimator that exploits the underlying spatial Poisson process related to the histogram explicitly when estimating the probability density with low-rank tensor decompositions or tensor completion. Furthermore, we demonstrate that our PTC estimator is a substantial improvement over standard histogram-based estimators for sub-Gaussian probability distributions because of the concentration of norm phenomenon.

The remainder of our paper is organized as follows: Sections 2 and 2.4 present the mathematical background and related work related to the PTC estimator. Section 3 provides a detailed description of the PTC estimator and a preliminary error analysis. Section 4 compares and demonstrates the improvements of the PTC estimator over existing estimators via several experiments. Conclusions and potential future work are presented in Section 5.

2 Background: frequency histograms, spatial Poisson processes, and count tensors

We first review the frequency histogram approximation of a d -variate density p under which the samples are independently drawn. We then demonstrate that the histogram counts can be identified with a spatial Poisson process and we can then conclude that the PTC estimator is a principled approach.

2.1 Frequency histograms

Suppose we have a collection of points

$$x_1, \dots, x_s \in \mathbb{R}^d \quad (2.1)$$

independently distributed with respect to a multivariate density p and then partition a finite volume

$$B = \bigcup_{j=1}^{n_1 n_2 \cdots n_d} B_j \subset \mathbb{R}^d \quad B_i \cap B_j = \emptyset \text{ when } i \neq j \quad (2.2)$$

where n_i is the number of bins along the i -th axis for $i = 1, \dots, d$ and denote

$$n := n_1 n_2 \cdots n_d$$

so that $|B| = \sum_{j=1}^n |B_j|$ is finite.

Let c_j denote the count of the points (2.1) that lie in bin B_j . The resulting frequency histogram can be normalized so that the approximation

$$\hat{p}_{\text{hist}} \mathbb{1}_B(x) := \sum_{j=1}^n \frac{c_j}{s|B_j|} \mathbb{1}_{B_j}(x) \approx p \mathbb{1}_B(x) \quad (2.3)$$

where $|B_j| = \int_{B_j} dV$ is the volume of B_j and the indicator function is defined by

$$\mathbb{1}_{B_j}(x) := \begin{cases} 1 & x \in B_j; \\ 0 & \text{otherwise} \end{cases}$$

holds over \mathbb{R}^d and implies that the error depends upon the size of $\hat{p}_{\text{hist}} - p$ over the finite volume region B and the size of p outside of B .

We can then approximate the differential entropy of random variable \mathbf{X} over region B

$$\text{ent}(p \mathbb{1}_B) = - \int_{B \subset \mathbb{R}^d} p \log p \, dV = \mathbb{E} \log p(\mathbf{X}) \mathbb{1}_B(\mathbf{X}) \quad (2.4)$$

with

$$\begin{aligned} \text{ent}(\widehat{p}_{\text{hist}} \mathbb{1}_B) &= - \sum_{j=1}^n \int_{B_j} \widehat{p}_{\text{hist}} \log \widehat{p}_{\text{hist}} \, dV \\ &= - \sum_{j=1}^n \frac{c_j}{s} \log \left(\frac{c_j}{m |B_j|} \right) \\ &= - \sum_{j=1}^n \frac{c_j}{s} \log \frac{c_j}{s} + \sum_{j=1}^n \frac{c_j}{s} \log |B_j|. \end{aligned} \quad (2.5)$$

Note that $\text{ent}(\widehat{p}_{\text{hist}} \mathbb{1}_B)$ remains well-defined for finite bin volumes $|B_j|$ and zero counts because $\lim_{x \rightarrow 0^+} x \log x = 0$.

2.2 Spatial Poisson processes

We now show that a useful model for the random set of points (2.1) is a spatial Poisson process. Define the counting measure

$$N(A) := \sum_{k=1}^s \mathbb{1}_A(x_k)$$

that returns the number of points (2.1) in $A \subset \mathbb{R}^d$ so that

$$N(B_j) = \sum_{k=1}^s \mathbb{1}_{B_j}(x_k) = c_j.$$

In words, the number of points in the frequency histogram bin B_j is given by $N(B_j)$. Well-known (see, e.g., [9, p.53]) is that the count c_j is binomially distributed with s events and success probability

$$\mu(B_j) = \int_{B_j} p \, dV. \quad (2.6)$$

Approximation of the Binomial distribution by the Poisson distribution is excellent when n is large and $\mu(B_j)$ is small so that the bin counts c_j can be approximated with a spatial Poisson process because the following two properties are satisfied:

1. For each bin B_j ,

$$\mathbb{P}[N(B_j) = k] = e^{-\mu(B_j)} \frac{(\mu(B_j))^k}{k!} \quad (2.7a)$$

where the success probability (2.6) is the mean measure for the spatial Poisson process and p can be identified with the Poisson intensity measure. This identification is the crucial relationship among the multivariate random variable density p , the Poisson intensity measure, and the spatial Poisson process that are leveraged by the PTC estimator.

2. Given the disjoint bins B_1, \dots, B_n , then

$$N(B_1), \dots, N(B_n) \quad (2.7b)$$

are independent random variables. This holds because we assumed that the set of points (2.1) are randomly drawn under p and we remark that the independence among the $N(B_j)$ holds regardless of the independence of variates.

2.3 Tensors

A tensor is multi-dimensional array where the order is the number of dimensions d . Examples include scalars (tensors of order zero), e.g., x ; vectors (tensors of order one), e.g., \mathbf{v} ; and matrices (tensors of order two), e.g., \mathbf{A} . Following tensor notation in [12], we denote tensors of order three and higher with bold capital script letters, e.g., $\mathbf{\mathcal{X}}$. The frequency histogram for the probability density p can be represented as a tensor of count data of order d , which we call the *histogram tensor*, with the partitioning scheme specified in (2.2). Unless the number of points (2.1) is exponentially large in the number of variates, an unlikely scenario, the histogram-based density estimator \hat{p}_{hist} is sparse with many zero or near-zero bins, and so does not provide an accurate approximation of the probability density so that the differential entropy approximation suffers. Exploiting this sparsity, we compute a low-rank Poisson canonical polyadic (CP) tensor decomposition [11] of the histogram tensor and use tensor completion to provide a model of the expected counts in all bins including those containing no sample points. We will show that for important classes of multivariate densities with appropriate tail behavior effecting concentration of norm, the density estimator based on the low-rank Poisson tensor decomposition and completion of the frequency histogram is an improvement over the histogram-based density estimator (2.3). The ensuing differential entropy estimator is an improvement, at times dramatically so, over the histogram-based differential entropy approximation (2.5).

As noted above, we develop our differential entropy estimator using the Poisson CP tensor decomposition. In future work, we may consider other low-rank tensor Poisson decompositions—e.g., Tucker [13] or tensor train [14] decompositions—when such models and associated statistical theory are adapted for use with Poisson data.

2.4 Related work

For a general survey of non-parametric entropy estimation, we refer the interested reader to [15]. We reviewed in Section 2 that the differential entropy of a random variable is a function of the corresponding probability density. Classical approaches to estimating the multivariate probability density include histograms and kernel density estimators (KDE) with the limitation that given s samples in d dimensions, consistency generally requires $sh^d \rightarrow \infty$, where h is the bin-width of the histogram or the bandwidth parameter for the KDE, see, e.g., the textbook [9] for a review. The authors of [10] introduce the use of tensor decompositions as an improvement on the histogram and KDE for high-dimensional density estimation. In contrast to our approach that only assumes the counts are independent (2.7b), the authors of [10] approach assumes independence of the variates and is equivalent to modeling the histogram counts as Gaussian data by using least-squares loss functions in computing the low-rank tensor decompositions. Three other papers [16, 17, 18] also use tensor decompositions to estimate a multivariate density. The report [17] is similar in spirit to that in [10], where a transformation into the Fourier domain leads to low-rank structure assumed in [19, 10]. The recent report [20] estimates multivariate intensity functions of spatial point processes using matrix- and tensor-based methods. Similarly, we note that our estimator is distinguished from these tensor-based estimators in that we model the histogram tensor values as counts and compute low-rank Poisson tensor factorizations to satisfy these modeling assumptions.

The accuracy of the histogram-based differential entropy estimator (2.5) depends upon an exponentially large number of bins with an increasing number of variates. The plug-in estimator

$$-\frac{1}{s} \sum_i \log \hat{p}_{\text{hist}}(x_i) \quad (2.8)$$

is simpler, however, its accuracy is also beholden to an exponential number of samples [21]. Our work directly improves upon the plug-in estimator (2.8) that is obtained with a histogram or KDE density estimate for a fixed sample size. A slight improvement to (2.8) might be obtained by splitting the data, that is, by using $s - 1$ points to estimate the density and then using the held-out point to estimate the entropy, before averaging over all held-out points, as in [22].

In one dimension, the inverse of the spacing between samples yields a rough estimate of the density at a given point, which can be used (with some bias-correction terms) in (2.8) [23]. In larger dimensions, the natural analog of the spacing estimator is based on the k -nearest neighbor distances. The work in [24] is such an estimator, which uses 1-nearest neighbor distances; later work, including [25] and [26] generalized the estimator to k -nearest neighbor distances for $k > 1$. We refer the interested reader to [27] and [28, 29] for a more thorough characterization of the spacing and k -NN estimators, respectively. In short, for s samples, we require k to be chosen so that $k/s \rightarrow 0$ for the estimator to be consistent, but $k \rightarrow \infty$ as a function of s for the variance to be minimized. estimator; a choice of $k_s \propto \log^6 s$ is sufficient. As a point of interest, the requirement that a density have at least one continuous derivative at all points (see [28, Theorem 1]) precludes the application of the above theory to the uniform distribution. A recent density estimator of non-trivial complexity is that in [30], which seeks to estimate a set of marginal distributions and

an accompanying copula or dependence structure of said marginals. The performance of this estimator is generally worse than the k -nearest neighbor (k -NN) distances [31], which is easily adapted to yield an estimator for the entropy and is based upon pairwise distances between samples. As we show in Section 4, our new PTC differential entropy estimator improves upon estimators based on these k -NN density approximations for several classes of probability distributions.

3 The Poisson tensor completion estimator for differential entropy

The histogram-based estimator $\text{ent}(\hat{p} \mathbb{1}_B)$ to $\text{ent}(p \mathbb{1}_B)$ in 2.5 is poor because the number of sample points in 2.1 needed for an acceptable approximation is prohibitive, especially when the dimension d increases because many bins will contain zero counts in which the contribution to the differential entropy is needed. In Section 2, we demonstrated the relationship among the frequency histogram, a spatial Poisson process modeling the sample points drawn from the d -variate distribution defined by density p , and an order- d tensor of counts. In this section, we leverage those relationships to define the *Poisson tensor completion (PTC)* estimator for differential entropy and demonstrate how it can be used for efficient estimation.

Tensor completion is a method for computing a low-rank model of tensor data given a sample of that data; see [32] and the references therein for an introduction to tensor completion and a survey of the many approaches developed. A standard approach to tensor completion is to compute a low-rank decomposition of the sampled data and then estimate the unobserved values in the tensor from that low-rank model. Here, we use that approach and compute a Poisson canonical polyadic (CP) tensor decomposition [11] of the histogram tensor, an approach novel with this paper.

We denote the histogram tensor for a d -variate density p defined over $n = n_1 n_2 \cdots n_d$ bins as $\mathcal{T} \in \mathbb{Z}_+^{n_1 \times n_2 \times \cdots \times n_d}$, where n_i is the number of bins into which dimension i is partitioned and \mathbb{Z}_+ is the set of nonnegative integers. Using multi-index notation to indicate a tensor element, i.e., $t_{\mathbf{i}} \equiv t_{i_1 i_2 \cdots i_d}$ denotes entry $\mathbf{i} = (i_1, \dots, i_d) \in [n_1] \otimes [n_2] \otimes \cdots \otimes [n_d]$ of \mathcal{T} with $[n_i] = \{1, \dots, n_i\}$, we model the elements of the histogram tensor as independent Poisson random variables

$$t_{\mathbf{i}} \sim \text{Poisson}(m_{\mathbf{i}}). \quad (3.1)$$

In other words, $t_{\mathbf{i}}$ is the number of samples x_i as defined in (2.1) that are located in bin B_{ℓ} for a unique linear index $\ell \in [n]$ so that the Poisson tensor assumption (3.1) is equivalent to the spatial Poisson process 2.7 modeling the bin counts. The linear index ℓ denotes a mapping between bin and tensor multi-indices and an example is the natural ordering index notation for tensors introduced in [33] where the relationship is $\ell = \mathbb{L}(\mathbf{i})$ and $\mathbf{i} = \mathbb{T}(\ell)$ and $\mathbb{L} : [n_1] \otimes \cdots \otimes [n_d] \mapsto \mathbb{Z}_+$ and $\mathbb{T} : \mathbb{Z}_+ \mapsto [n_1] \otimes \cdots \otimes [n_d]$.

To the best of our knowledge, we are the first to identify the relationship between a spatial Poisson process and a Poisson canonical polyadic (CP) tensor decomposition [11] to model histogram bin counts. We also remark that \mathcal{T} will contain many entries corresponding to unobserved or low counts unless the number of samples s is exponentially large in the number of dimensions (i.e. variates) d . Poisson tensor completion is a mechanism for imputing the expected values for these entries under the Poisson assumption (3.1).

We complete \mathcal{T} by imposing low-rank CP structure on the corresponding Poisson parameter tensor

$$\mathcal{M} := \sum_{r=1}^R \lambda_r \mathbf{a}_r^{(1)} \circ \mathbf{a}_r^{(2)} \circ \cdots \circ \mathbf{a}_r^{(d)} \in \mathbb{R}_+^{n_1 \times n_2 \times \cdots \times n_d}, \quad (3.2)$$

where \circ denotes the outer product of two vectors, $\|\mathbf{a}_r^{(i)}\|_1 = 1, \forall i \in \{1, \dots, d\}, \forall r \in \{1, \dots, R\}$, and \mathbb{R}_+ is the set of nonnegative real values. Note that the entries $m_{\mathbf{i}}$ of the low-rank CP parameter tensor \mathcal{M} are nonnegative because, by definition, they model the probability of a number of events occurring in a bounded region of \mathbb{R}^d as defined by the spatial Poisson process associated with the frequency histogram discussed in §2. This approach is an alternative [10, 20], which relies on tensor decompositions designed for Gaussian data and does not guarantee nonnegative entries without imposing additional constraints.

Let $m_{\mathbf{i}}$ is the \mathbf{i} entry of the rank R tensor \mathcal{M} . We estimate the mean measure (2.6) of the spatial Poisson process using the maximum Poisson likelihood estimation

$$\widehat{\mathcal{M}} = \arg \max_{\mathbf{i}=(1,1,\cdots,1)} \sum_{(n_1,n_2,\cdots,n_d)} (m_{\mathbf{i}} - t_{\mathbf{i}} \log m_{\mathbf{i}}) \quad (3.3)$$

as introduced in [11]. Then, with the natural ordering index mapping \mathbb{T} defined above, each entry in $\widehat{\mathcal{M}}$ estimates the true Poisson parameter of (3.1), which in turn represents the expected count of the corresponding bin in the

frequency histogram as follows:

$$\widehat{m}_{\mathbb{T}(\ell)} = \widehat{m}_i \approx m_i = \mathbb{E}(t_i) . \quad (3.4)$$

We can therefore denote the induced probability density

$$\widehat{p}_{\text{ptc}} \mathbb{1}_B := \frac{1}{\|\widehat{\mathcal{M}}\|_1} \sum_{j=1}^n \frac{\widehat{m}_{\mathbb{T}(j)}}{|B_j|} \quad (3.5a)$$

where $\|\widehat{\mathcal{M}}\|_1 := \sum_{j=1}^n \widehat{m}_{\mathbb{T}(j)}$ so that

$$(\widehat{p}_{\text{ptc}} \mathbb{1}_B)(x) = \begin{cases} \frac{\widehat{m}_{\mathbb{T}(j)}}{\|\widehat{\mathcal{M}}\|_1 |B_j|} & x \in B_j \\ 0 & x \notin B_j . \end{cases} \quad (3.5b)$$

For a real-valued function $f : \mathbb{R}^d \rightarrow \mathbb{R}$, we then have that

$$\int_{\mathbb{R}^d} f \widehat{p}_{\text{ptc}} \mathbb{1}_B dV = \int_B f \widehat{p}_{\text{ptc}} dV = \sum_{j=1}^n \int_{B_j} f \widehat{p}_{\text{ptc}} dV = \frac{1}{\|\widehat{\mathcal{M}}\|_1} \sum_{j=1}^n \widehat{m}_{\mathbb{T}(j)} \bar{f}_{B_j}$$

where $\bar{f}_{B_j} := \frac{1}{|B_j|} \int_{B_j} f dV$ is the average value of f over the bin B_j . In so many words, *the frequency histogram for samples of a multivariate probability density p with d variates can be identified with an estimate of the mean measure of the spatial Poisson process, $\widehat{\mathcal{M}}$, computed via Poisson tensor completion.* Setting $f = \log(\widehat{p}_{\text{ptc}} \mathbb{1}_B)$ defines the PTC estimator for differential entropy as

$$\text{ent}(\widehat{p}_{\text{ptc}} \mathbb{1}_B) = - \sum_{j=1}^n \frac{\widehat{m}_{\mathbb{T}(j)}}{\|\widehat{\mathcal{M}}\|_1} \log \left(\frac{\widehat{m}_{\mathbb{T}(j)}}{\|\widehat{\mathcal{M}}\|_1 |B_j|} \right) \quad (3.6)$$

because $\bar{f}_{B_j} = \log \left(\frac{\widehat{m}_{\mathbb{T}(j)}}{\|\widehat{\mathcal{M}}\|_1 |B_j|} \right)$.

Our estimate of the underlying multivariate density is given by the dense tensor $\widehat{\mathcal{M}}$ that is the same size as the histogram tensor \mathcal{T} , which contains $\prod_{i=1}^d n_i$ entries and subject to the available computation resources, may be prohibitively too large to store. Thus, it is useful to store $\widehat{\mathcal{M}}$ in its decomposed form defined in (3.2), which is comprised of $(R+1) \sum_{i=1}^d n_i$ entries, computing $\|\widehat{\mathcal{M}}\|_1$ and $\widehat{m}_{\mathbb{T}(j)}$ in (3.6) only as needed. Recall that the vectors of a Poisson CP tensor decomposition (3.2) are normalized to unit length in the 1-norm, thus leading to the simple computation $\|\widehat{\mathcal{M}}\|_1 = \sum_{r=1}^R \lambda_r$. Computing each $\widehat{m}_{\mathbb{T}(j)}$ requires $R(d+1)$ operations.

3.1 Error Analysis

The error of PTC entropy estimator is

$$\begin{aligned} \text{ent}(\widehat{p}_{\text{ptc}}) - \text{ent}(p) &= \text{ent}(\widehat{p}_{\text{ptc}} \mathbb{1}_B) - \text{ent}(p \mathbb{1}_B) - \text{ent}(p \mathbb{1}_{\mathbb{R}^d \setminus B}) \\ &= - \sum_{j=1}^n \int_B (\widehat{p}_{\text{ptc}} \log(\widehat{p}_{\text{ptc}}) - p \log(p)) \mathbb{1}_{B_j} dV - \text{ent}(p \mathbb{1}_{\mathbb{R}^d \setminus B}) \\ &= - \sum_{j=1}^n \left(\frac{\widehat{m}_{\mathbb{T}(j)}}{\|\widehat{\mathcal{M}}\|_1} \log \left(\frac{\widehat{m}_{\mathbb{T}(j)}}{\|\widehat{\mathcal{M}}\|_1 |B_j|} \right) - \int_{B_j} p \mathbb{1}_{B_j} \log(p \mathbb{1}_{B_j}) dV \right) - \text{ent}(p \mathbb{1}_{\mathbb{R}^d \setminus B}) \quad (3.7a) \end{aligned}$$

and an analogous estimate for the histogram error is

$$\begin{aligned} \text{ent}(\widehat{p}_{\text{hist}}) - \text{ent}(p) &= - \sum_{j=1}^n \left(\frac{c_j}{s} \mathbb{1}_{B_j} \log \left(\frac{c_j}{s |B_j|} \mathbb{1}_{B_j} \right) - \int_{B_j} p \mathbb{1}_{B_j} \log(p \mathbb{1}_{B_j}) dV \right) \\ &\quad - \text{ent}(p \mathbb{1}_{\mathbb{R}^d \setminus B}) . \quad (3.7b) \end{aligned}$$

where recall that s is the number of samples and c_j is count of samples in bin B_j , which is binomially distributed and we model with a spatial Poisson process, see the discussion following (2.6). Both estimates enables us to conclude

that error can be no larger than the size of p on $\mathbb{R}^d \setminus B$. This, for example suggests that the tail behavior of p plays a crucial role independent of the estimator. The estimators differ in their bin-wise expressions and consists of the error in density estimation and then entropy estimation. The value of $\text{ent}(\widehat{p}_{\text{hist}})$ over bins without counts is zero whereas $\text{ent}(\widehat{p}_{\text{ptc}})$ is non-zero because of tensor completion. The bias-variance tradeoff for the size of the bins for a histogram density estimator is well-known, see, e.g., [9] reviewing that decreasing bin size increases the variance and increasing bin size increases the bias. However the bias-variance tradeoff for bin sizes of PTC density estimation is nontrivial because as we explained in the paragraph containing (3.4) the tensor $\widehat{\mathcal{M}}$ is determined by a maximum Poisson likelihood estimation introduced in [11]. This likelihood approach was introduced as a loss function for an optimization algorithm to approximate the Poisson parameters $m_i = \mathbb{E}(t_i)$ —the bias and variance of $\widehat{\mathcal{M}}$ was not considered. In addition, the propagation of the error in completion to the error in entropy approximation requires investigation.

The comparison of the bin-wise error suggests that distributions with many bins with zero or near-zero counts are ripe to reap the rewards of completion (and the numerical results in §4.1 will confirm this). Such distributions enable a tremendous amount of tensor completion. Such a trend, as it turns out, is generic for the important class of sub-gaussian distributions as we now review. The random vector $\mathbf{X} \in \mathbb{R}^d$ has sub-gaussian components X_i when

$$\mathbb{P}\{|X_i| \geq t\} \leq 2e^{-ct^2} \quad (3.8a)$$

for a constant c and $i = 1, \dots, d$. In words, the tails of the multivariate distribution for X decay as for a multivariate normal distribution. Examples of sub-gaussian distributions include Gaussians, uniform, bounded distributions and mixtures of sub-gaussian distributions. An important consequence is that for such distributions there is a concentration of norm, i.e.,

$$\mathbb{P}\{\|\mathbf{X}\|_2 - \sqrt{d} \geq t\} \leq 2e^{-\tilde{c}t^2} \quad (3.8b)$$

where $\|\mathbf{X}\|_2 = \sqrt{\sum_{i=1}^d X_i^2}$ and a constant \tilde{c} . In particular, a sample of a multivariate standard normal concentrates about a thin spherical shell of radius \sqrt{d} so that as the number of variates d increases so does the distance of the spherical shell from the origin. This suggests a threshold on the size of the elements of $\widehat{\mathcal{M}}$ during the computation of $\widehat{\mathcal{M}}$ and such a scheme is introduced §4.3.

4 Experiments

Our experiments were performed in Python and are summarized by the following three steps.

1. Sample the appropriate distribution p to generate s random points (2.1).
2. Bin the random points according to a specified binning scheme. Use a sparse representation of the histogram, keeping track of the nonempty bins, counts, and bin volumes. Unless otherwise specified:
 - estimates of differential entropy from s samples of a d -dimensional distribution made using a histogram directly used bins of width

$$3.5s^{-\frac{1}{d+2}} \text{ in each dimension so that } |B_j| = (3.5)^d s^{-\frac{d}{d+2}} \quad (4.1)$$

where s is the number of samples. We selected this value to be close to the asymptotically optimal bin widths for the multivariate Gaussian $N(0_d, I_d)$, [9, Eq. (3.66)]. The bin edges can be found using, e.g., `arange` from `numpy` [34].

- histogram tensors have $n_i = 20$ in each dimension for a total of $n = 20^d$ bins. The bin edges can be found using, e.g., `histogram_bin_edges` from `numpy`.
- 3. Use the routines `sptensor.from_data` and `cp_apr` in the Tensor Toolbox `pyttb` [35] to compute the low-rank Poisson CP tensor model $\widehat{\mathcal{M}}$ as in (3.2). Unless otherwise specified, the experiments used rank R at most 5.

Our experiments investigate the effect of bin size when the entropy of the underlying density is known in §4.1 and then in §4.2 we use a Gaussian mixture model, which does not have a closed-form expression for the entropy, to understand the role of rank selection. Because the entropy is small where the density is small, then we introduce a simple thresholding in §4.3 on the size of the entries of $\widehat{\mathcal{M}}$ to reduce the cost, which becomes prohibitive with an increasing number of variates d because $\widehat{\mathcal{M}}$ cannot be formed without a significant amount of memory nor can we compute the individual elements $\widehat{m}_{\mathbb{T}(j)}$ without a significant amount of computation.

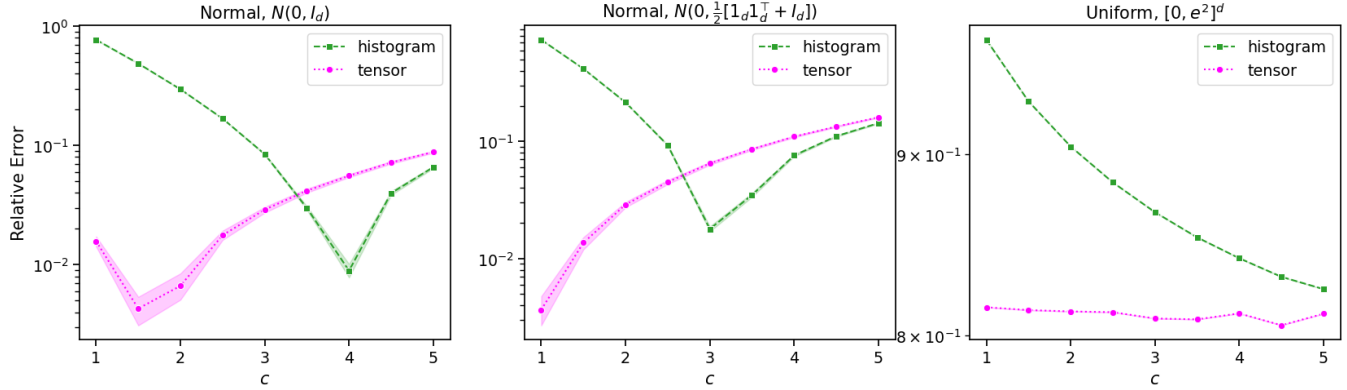


Figure 1: Comparing estimates and bins used from 25 trials for dimension 6 distributions. The histogram is constructed by placing $s = 2500$ samples from the distributions into bins of width $c s^{-\frac{1}{8}}$ in each dimension, for different values of c . Here, the tensor-based approximation uses the same bins as the histogram-based approximation.

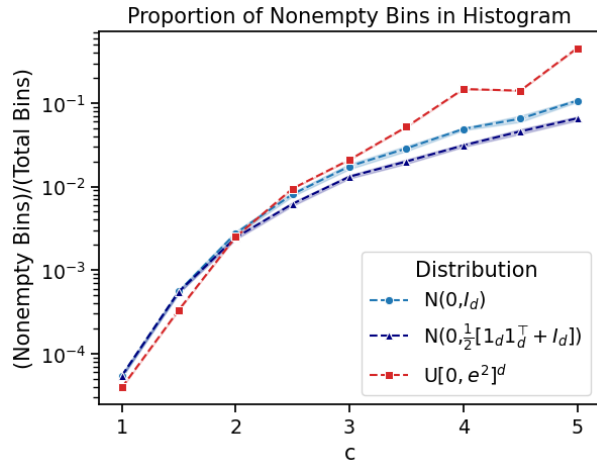


Figure 2: The proportion of nonempty bins for the histograms used to estimate entropy in Figure 1. The distributions are dimension $d = 6$, and the histograms use bins of width $c \cdot (2500)^{-\frac{1}{8}}$ in each dimension, for different values of c . As c increases, the number of bins decreases.

4.1 Bin width

In order to determine the influence of bin width, we select two multivariate normal distributions and multivariate uniform distributions with independent variates, each with closed-form formulas for the entropy so that we can determine the relative error in the approximation. The multivariate normal distribution has entropy $d/2 \log(2\pi e) + 1/2 \log \det \Sigma$ where Σ is the covariance matrix of order d and the entropy for a multivariate uniform distributions with independent variates is $\log(b_1 - a_1) \cdots \log(b_d - a_d)$ where the univariate distribution for the i -th variate is over the interval (a_i, b_i) . Figure 1 shows that larger bin size favor the histogram-based entropy estimates and smaller bin sizes favor the tensor-based entropy estimates, and the difference is nearly two-orders of magnitude for smallest bin sizes. Figure 2 shows the proportion of nonempty bins for the binning schemes in Figure 1 with the fraction of nonempty bins occupied differing by four orders of magnitude. The two figures suggest that increasing the number of bins decreases the fraction of bins with positive counts and so favors the tensor-based entropy estimates. The figures also imply that tensor completion effected has a dramatic impact upon the relative accuracy. The three distributions are examples of sub-gaussian distributions reviewed at the end of §3 and demonstrate that tensor completion favors a binning scheme with small sized bins in contrast to the histogram estimator of the entropy.

Figures 3 and 4 show a comparison of the error in estimating differential entropy using a histogram directly, using a low-rank tensor approximation to a histogram, or using the k-NN method for several multivariate distributions with dimension 5. In these plots we observe that the PTC estimator outperforms the k-NN estimator for the uniform distribution on $[0, 1]^d$, the two methods are similar (within an order of magnitude) for normal distributions and the

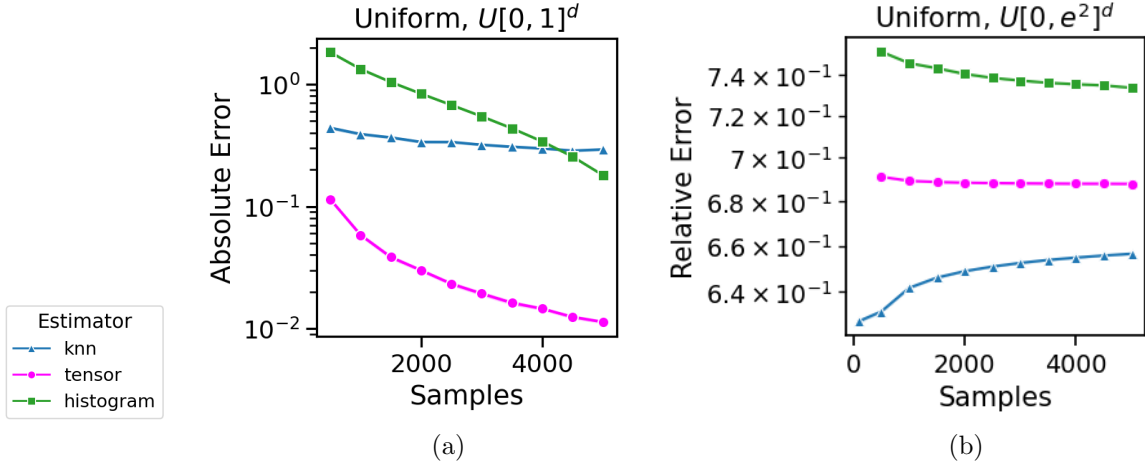


Figure 3: Error in estimated entropy of a uniform distribution over (a) $[0, 1]^5$ or (b) $[0, e^2]^5$ with independent dimensions. Estimates use a histogram directly, the tensor method, or the k -NN method. The results shown are for dimension 5 over 25 trials using the $k \in \{1, 2, 3, \dots, 10, 25, 50, 100, 200\}$ or rank ≤ 5 leading to the smallest error.

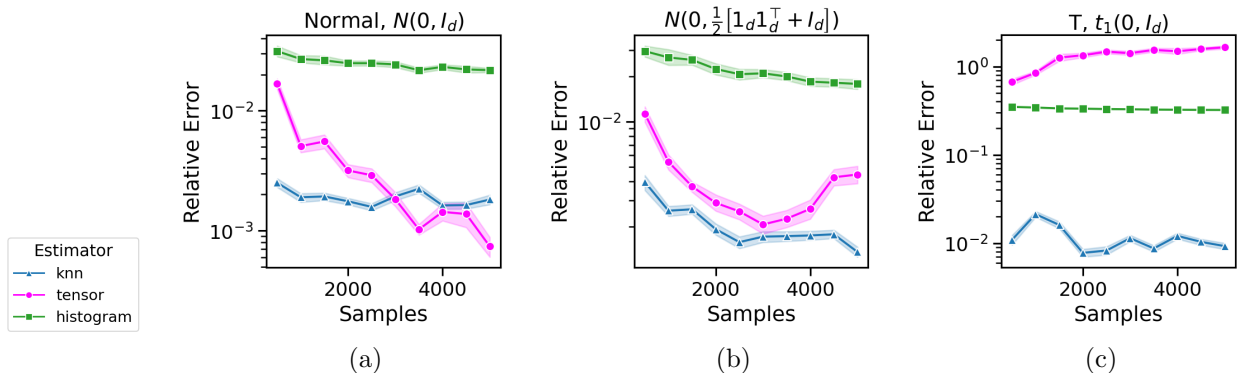


Figure 4: Error in estimated entropy using a histogram directly, the tensor method, or using the k -NN method. The results shown are for dimension 5, over 25 trials using the $k \in \{1, 2, 3, \dots, 10, 25, 50, 100, 200\}$ or rank ≤ 5 leading to the smallest error. The distributions shown are (a) Normal with independent dimensions (b) Normal with correlation between dimensions, and (c) t with one degree of freedom and independent dimensions (equivalent to a Cauchy distribution).

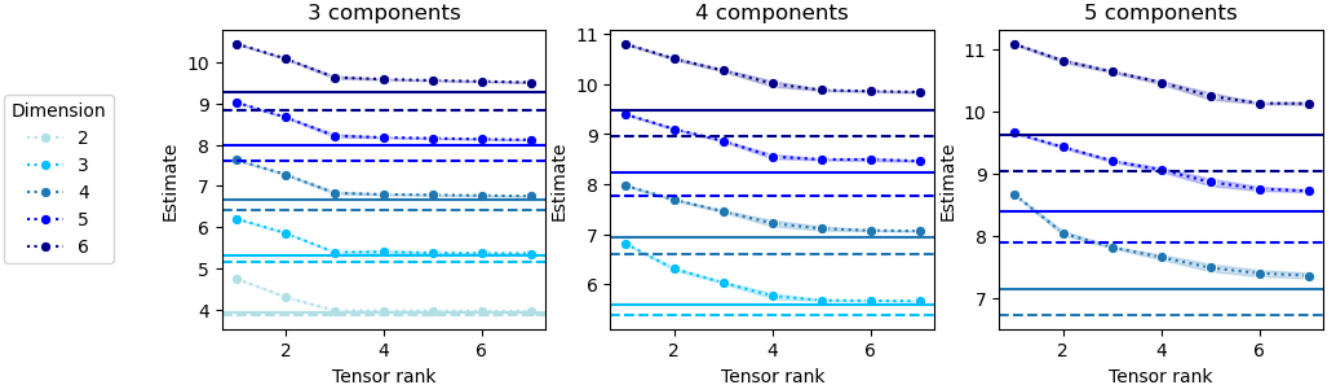


Figure 5: Estimated entropy for Gaussian mixtures with 3, 4, and 5 components. Dotted lines: tensor estimates from 25 trials of $s = 2,500$ samples from the distribution. Dashed lines: average histogram estimate in 25 trials of 2,500 samples. Solid lines: average histogram estimate in 25 trials with $s = 1,000,000$ samples.

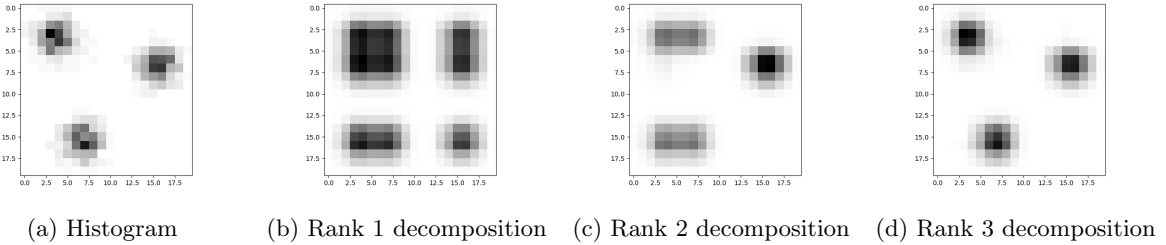


Figure 6: Plots of a histogram of 1000 samples from two-dimensional Gaussian mixture with three equidistant modes and its rank 1, 2, and 3 tensor decompositions.

uniform distribution on $[0, e^2]^d$, and the k-NN estimator outperforms the tensor-based estimator for the heavy-tailed Cauchy distribution. The poor behavior of PTC on the heavy-tailed Cauchy distribution and excellent behavior of PTC on sub-gaussian distributions suggests that an adequate number of samples in a small number of bins is important attribute.

4.2 Gaussian Mixtures

Figure 5 shows the estimated entropy for different tensor ranks compared to estimates from histograms with the $s = 2,500$ samples and estimates from histograms with s equal to one million samples for three Gaussian mixtures with three, four and five components. The bin sizes for the histogram is given by (4.1) and the binning for the tensor estimates uses 20 bins in each direction. The large sample histogram provides a basis of comparison because there is no closed form expression for the entropy of a Gaussian mixture with more than one component. We conclude that the tensor rank R needs to equal the number of components and that PTC increases in accuracy over the histogram estimate as the number of variates increases. The latter accuracy allows us to conclude that PTC leads to a more accurate estimate with a fixed sample size.

A practical detail associated with PTC is the selection of the rank R needed for $\widehat{\mathcal{M}}$. There is little theory to guide us and determining R depends upon the application. The number of components of the mixture provides a clue. We observe a relationship between the number of mixture components and the tensor rank used to estimate the entropy. Figure 6 shows pictures of the tensor decompositions of a histogram for a two-dimensional Gaussian mixture with three components. The sequence suggests that the rank R needs to be as least as large as the number of components.

Denote each of the R rank-one matrices in (3.2) by $\widehat{\mathcal{M}}_r$ so that $\widehat{\mathcal{M}} = \sum_{r=1}^R \widehat{\mathcal{M}}_r$ and let $\widehat{\mathcal{N}}$ be the tensor of order

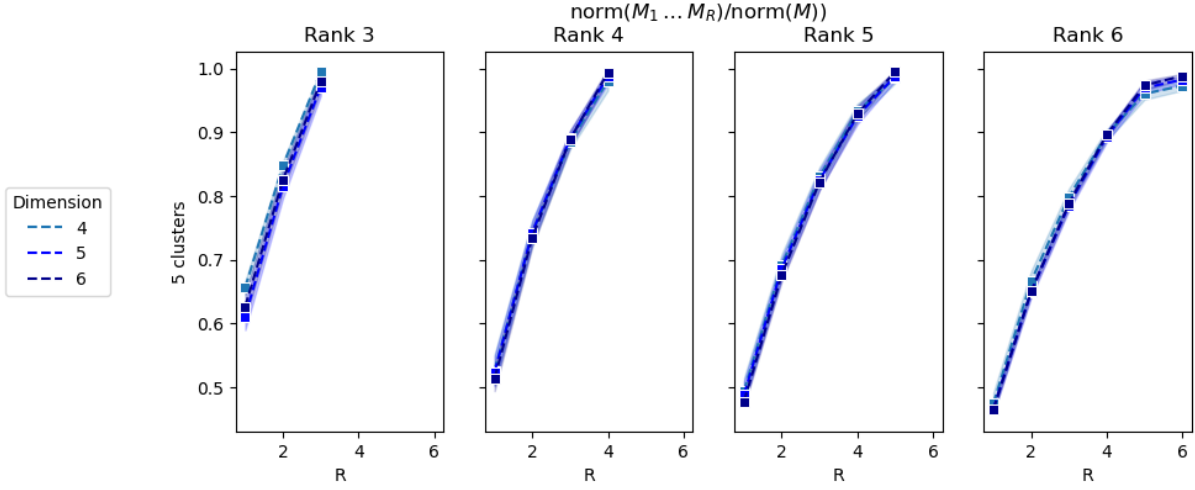


Figure 7: $\frac{\|\text{vec}(\widehat{\mathcal{M}}_1) \cdots \text{vec}(\widehat{\mathcal{M}}_R)\|_F}{\|\widehat{\mathcal{M}}\|_F}$ for components $\widehat{\mathcal{M}}_R$ of tensor $\widehat{\mathcal{M}}$ from 25 trials of 2500 samples from Gaussian mixtures with 5 clusters.

$d + 1$ with dimensions $R \times n_1 \times n_2 \times \cdots \times n_d$. Each subplot of Figure 7 plots the ratio

$$\begin{aligned} \rho_k &:= \frac{\|\begin{bmatrix} \text{vec}(\widehat{\mathcal{M}}_1) & \cdots & \text{vec}(\widehat{\mathcal{M}}_k) \end{bmatrix}\|_F}{\|\widehat{\mathcal{M}}\|_F} = \frac{\|\begin{bmatrix} \widehat{\mathcal{N}}_{(1)}^\top \mathbf{e}_1 & \cdots & \widehat{\mathcal{N}}_{(1)}^\top \mathbf{e}_k \end{bmatrix}^\top\|_F}{\|\widehat{\mathcal{N}}\|_F} \\ &= \frac{\|\begin{bmatrix} \widehat{\mathcal{N}}_{(1)}^\top \mathbf{e}_1 & \cdots & \widehat{\mathcal{N}}_{(1)}^\top \mathbf{e}_k \end{bmatrix}\|_F}{\|\widehat{\mathcal{N}}\|_F} \end{aligned}$$

for $k = 1, \dots, R$ and $\widehat{\mathcal{N}}_{(1)}$ is the matricization of $\widehat{\mathcal{N}}$ along the first dimension. Note that the r -th row of matrix $\widehat{\mathcal{N}}_{(1)}$ is denoted by $\mathbf{e}_r^\top \widehat{\mathcal{N}}_{(1)} = (\widehat{\mathcal{N}}_{(1)}^\top \mathbf{e}_r)^\top$ and equals $\text{vec}(\widehat{\mathcal{M}}_r)$ so that the above ratio determines the amount of linear independence in the first k rows of $\widehat{\mathcal{N}}_{(1)}$. Equivalently, the ratio indicates whether there is a value of k such that tensor $\sum_{r=1}^k \widehat{\mathcal{M}}_r \approx \widehat{\mathcal{M}}$ and note that the ratio is unity for $k = R$. In Figure 7, we observe that a noticeable change occurs close to where the rank of the decomposition matches the number of components in the mixture.

4.3 Tensor Thresholding

A useful observation is that the Rd vectors $\widehat{\mathbf{a}}_r^{(i)}$ in the Poisson CP estimator $\widehat{\mathcal{M}}$ of the model defined in (3.2) are non-negative and can be identified with a probability mass function. In particular, the non-negative elements are no larger than one. Hence, the small elements of $\mathbf{a}_r^{(j)}$ imply that the corresponding elements in the rank-one tensor

$$\widehat{\mathcal{M}}_r := \lambda_r \widehat{\mathbf{a}}_r^{(1)} \circ \widehat{\mathbf{a}}_r^{(2)} \circ \cdots \circ \widehat{\mathbf{a}}_r^{(d)}$$

are also small and have negligible contribution to $\text{ent}(\widehat{p}_{\text{ptc}} \mathbf{1}_B)$. For example, if the first element of $\widehat{\mathbf{a}}_r^{(1)}$ is small, then $n_2 n_3 \cdots n_d$ elements of the r -th rank-one tensor of $\widehat{\mathcal{M}}$ are also small. This corresponds to a sub-tensor of order $d - 1$ for the r -th rank-one tensor corresponding to $\widehat{\mathbf{a}}_r^{(1)}$. This suggests a simple thresholding algorithm, that can be used to approximate the estimator in (3.6) and thus lower the memory and computational requirements:

- Determine the Rd sets $\Omega_{r,i}$ containing the indices for each of the Rd vectors $\widehat{\mathbf{a}}_r^{(i)}$ where the elements are less than a threshold $0 < \tau < 1$. Approximate $\text{ent}(\widehat{p}_{\text{ptc}} \mathbf{1}_B)$ using the elements of $\widehat{\mathcal{M}}$ not containing any of the $\sum_{r=1}^R \sum_{i=1}^d \Omega_{r,i}$ indices. The number of elements in the sum of the R rank-one tensors is Rn . If $|\Omega_{r,i}|$ denotes the number of indices in $\Omega_{r,i}$, then

$$Rn - \sum_{r=1}^R \sum_{i=1}^d |\Omega_{r,i}| \frac{n}{n_i}$$

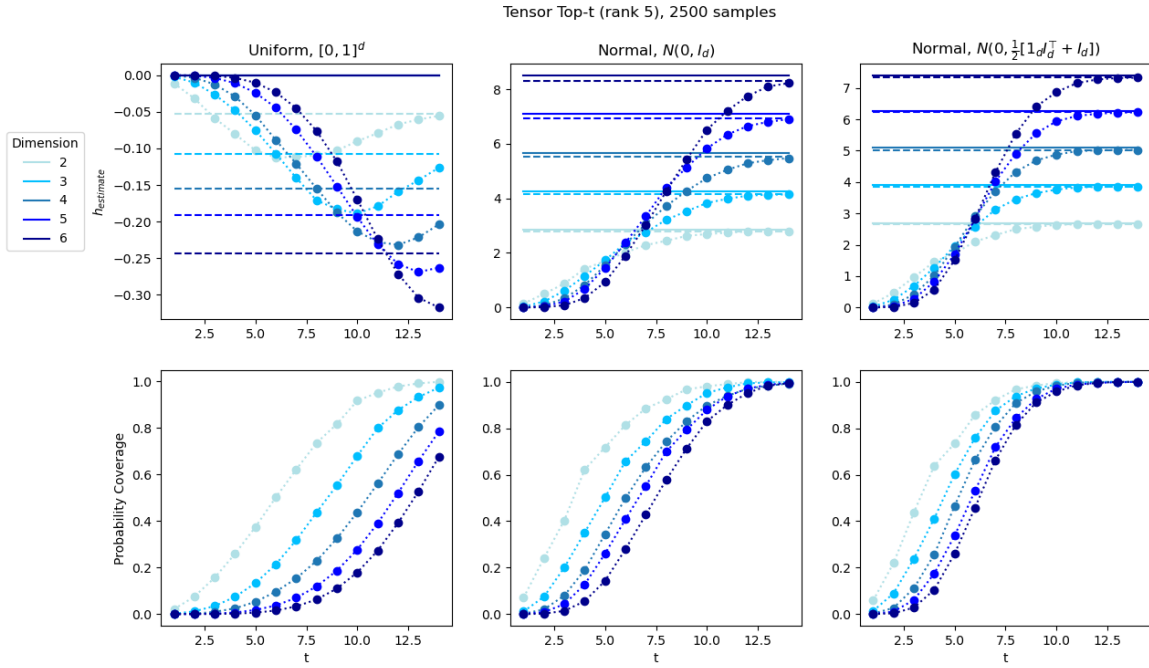


Figure 8: Tensor top- t sampling. The first row shows the entropy estimates using a sample of a tensor. Solid lines show the true entropy and dashed lines show the (full) rank 5 tensor estimate. The second row shows the portion of the sum of values in the tensor accounted for through sampling the tensor.

is the number of elements needed to approximate $\text{ent}(\hat{p}_{\text{ptc}} \mathbf{1}_B)$. The number of non-negligible elements can be as small as zero when $|\Omega_{r,i}| = n_i$ and as large as Rn when $|\Omega_{r,i}| = 0$. Note that $|\Omega_{r,i}| = n_i$ occurs when $\hat{\mathbf{a}}_r^{(i)}$ is a uniform distribution (or nearly so) and $\tau n_i > 1$.

Figure 8 shows entropy estimates found by sampling a tensor for the uniform distribution on $[0, 1]^d$ and normal distributions $N(0, I_d)$ and $N(0, \frac{1}{2}[1_d I_d^T + I_d])$. The estimate to the tensor found by combining the top- t indices approaches the estimate found using the full tensor for increasing t .

5 Conclusion

We introduced the non-parametric *Poisson tensor completion (PTC) estimator* (3.6) using the low-rank Poisson tensor $\widehat{\mathcal{M}}$ to approximate the entropy estimator for a multivariate random variable from a frequency histogram. The PTC estimator leverages the inter-sample relationships determined during a maximum Poisson likelihood estimation introduced in [11] to compute a low-rank Poisson tensor decomposition of the frequency histogram. Our crucial observation is that the histogram bins are an instance of a space partitioning of counts and thus can be identified with a spatial Poisson process. The Poisson tensor decomposition leads to a completion of the intensity measure over all bins—including those containing few to no samples—and leads to our proposed PTC differential entropy estimator. An error analysis underscored the role played by the tensor completion to impute values for the density and numerical experiments examined the role of sub-gaussian distribution, thresholding and the determination of tensor rank. PTC appears to work well on sub-gaussian distributions because when there is an adequate number of samples in a small number of bins.

Our future work consists in determining the approximation provided by tensor completion and appropriate binning strategies. Our previous work on Poisson tensor completion demonstrated that a zero-truncated Poisson CP decomposition [36] can better estimate expected counts than when using a Poisson CP decomposition if the number of zero counts in the observed tensor is not too large relative to the sizes of the dimensions of the tensor. We plan to explore the conditions where such a result combined with the thresholding approach above may lead to an even more efficient estimator for sub-gaussian distributions based on zero-truncated Poisson tensor completion.

Acknowledgments

We thank Derek Tucker of Sandia National Labs for several helpful discussions during the writing of this manuscript. The second author thanks Scott McKinley of Tulane University for several helpful discussions on spatial Poisson Processes. This work was supported by the Laboratory Directed Research and Development program (Project 233076) at Sandia National Laboratories, a multimission laboratory managed and operated by National Technology and Engineering Solutions of Sandia LLC, a wholly owned subsidiary of Honeywell International Inc. for the U.S. Department of Energy's National Nuclear Security Administration under contract DE-NA0003525.

References

- [1] D. Gokhale, “On entropy-based goodness-of-fit tests,” *Computational Statistics & Data Analysis*, vol. 1, pp. 157–165, 1983.
- [2] E. Parzen, “Goodness of fit tests and entropy,” *Journal of Combinatorics, Information, and System Science*, vol. 16, pp. 129–136, 1991.
- [3] R. Cheng and N. Amin, “Estimating parameters in continuous univariate distributions with a shifted origin,” *Journal of the Royal Statistical Society: Series B (Methodological)*, vol. 45, no. 3, pp. 394–403, 1983.
- [4] S. Zhu, D. Wang, K. Yu, T. Li, and Y. Gong, “Feature selection for gene expression using model-based entropy,” *IEEE/ACM Transactions on Computational Biology and Bioinformatics*, vol. 7, no. 1, pp. 25–36, 2008.
- [5] A. Hyvärinen, “New approximations of differential entropy for independent component analysis and projection pursuit,” *Advances in neural information processing systems*, vol. 10, 1997.
- [6] L. Faivishevsky and J. Goldberger, “Ica based on a smooth estimation of the differential entropy,” *Advances in neural information processing systems*, vol. 21, 2008.
- [7] S. Talukdar, S. Bhaban, and M. V. Salapaka, “Memory erasure using time-multiplexed potentials,” *Physical Review E*, vol. 95, no. 6, p. 062121, 2017.
- [8] Y. Han, J. Jiao, T. Weissman, and Y. Wu, “Optimal rates of entropy estimation over lipschitz balls,” *The Annals of Statistics*, vol. 48, no. 6, pp. 3228–3250, 2020.
- [9] D. Scott, *Multivariate Density Estimation: Theory, Practice, and Visualization*, ser. A Wiley-interscience publication. Wiley, 2015.
- [10] R. A. Vandermeulen and A. Ledent, “Beyond smoothness: Incorporating low-rank analysis into nonparametric density estimation,” *Advances in Neural Information Processing Systems*, vol. 34, pp. 12180–12193, 2021.
- [11] E. C. Chi and T. G. Kolda, “On tensors, sparsity, and nonnegative factorizations,” *SIAM Journal on Matrix Analysis and Applications*, vol. 33, no. 4, pp. 1272–1299, 2012.
- [12] T. G. Kolda and B. W. Bader, “Tensor decompositions and applications,” *SIAM Review*, vol. 51, no. 3, pp. 455–500, Sep. 2009.
- [13] L. R. Tucker, “Some mathematical notes on three-mode factor analysis,” *Psychometrika*, vol. 31, pp. 279–311, 1966.
- [14] I. V. Oseledets, “Tensor-train decomposition,” *SIAM Journal on Scientific Computing*, vol. 33, no. 5, pp. 2295–2317, 2011.
- [15] J. Beirlant, E. J. Dudewicz, L. Györfi, E. C. Van der Meulen *et al.*, “Nonparametric entropy estimation: An overview,” *International Journal of Mathematical and Statistical Sciences*, vol. 6, no. 1, pp. 17–39, 1997.
- [16] M. Amiridi, N. Kargas, and N. D. Sidiropoulos, “Information-theoretic feature selection via tensor decomposition and submodularity,” *Trans. Sig. Proc.*, vol. 69, p. 6195–6205, Jan. 2021. [Online]. Available: <https://doi.org/10.1109/TSP.2021.3125147>
- [17] ———, “Low-rank characteristic tensor density estimation part i: Foundations,” *IEEE Transactions on Signal Processing*, vol. 70, pp. 2654–2668, 2022.

[18] ——, “Low-rank characteristic tensor density estimation part ii: Compression and latent density estimation,” *IEEE Transactions on Signal Processing*, vol. 70, pp. 2669–2680, 2022.

[19] R. A. Vandermeulen, “Improving nonparametric density estimation with tensor decompositions,” 2020. [Online]. Available: <https://arxiv.org/abs/2010.02425>

[20] H. Xu, C. M. M. Padilla, O. H. M. Padilla, and D. Wang, “Multivariate Poisson intensity estimation via low-rank tensor decomposition,” 2025. [Online]. Available: <https://arxiv.org/abs/2504.15879>

[21] H. Joe, “Estimation of entropy and other functionals of a multivariate density,” *Annals of the Institute of Statistical Mathematics*, vol. 41, pp. 683–697, 1989.

[22] P. Hall and S. C. Morton, “On the estimation of entropy,” *Annals of the Institute of Statistical Mathematics*, vol. 45, pp. 69–88, 1993.

[23] F. Tarasenko, “On the evaluation of an unknown probability density function, the direct estimation of the entropy from independent observations of a continuous random variable, and the distribution-free entropy test of goodness-of-fit,” *Proceedings of the IEEE*, vol. 56, no. 11, pp. 2052–2053, 1968.

[24] L. F. Kozachenko and N. N. Leonenko, “Sample estimate of the entropy of a random vector,” *Problemy Peredachi Informatsii*, vol. 23, no. 2, pp. 9–16, 1987.

[25] H. Singh, N. Misra, V. Hnizdo, A. Fedorowicz, and E. Demchuk, “Nearest neighbor estimates of entropy,” *American journal of mathematical and management sciences*, vol. 23, no. 3-4, pp. 301–321, 2003.

[26] M. N. Goria, N. N. Leonenko, V. V. Mergel, and P. L. Novi Inverardi, “A new class of random vector entropy estimators and its applications in testing statistical hypotheses,” *Journal of Nonparametric Statistics*, vol. 17, no. 3, pp. 277–297, 2005.

[27] P. Hall, “Limit theorems for sums of general functions of m-spacings,” in *Mathematical Proceedings of the Cambridge Philosophical Society*, vol. 96, no. 3. Cambridge University Press, 1984, pp. 517–532.

[28] T. B. Berrett, R. J. Samworth, and M. Yuan, “Efficient multivariate entropy estimation via k -nearest neighbour distances,” *The Annals of Statistics*, vol. 47, no. 1, pp. 288–318, 2019.

[29] R. Mnatsakanov, N. Misra, S. Li, and E. Harner, “ k_n -nearest neighbor estimators of entropy,” *Mathematical Methods of Statistics*, vol. 17, pp. 261–277, 2008.

[30] G. Ariel and Y. Louzoun, “Estimating differential entropy using recursive copula splitting,” *Entropy*, vol. 22, no. 2, p. 236, 2020.

[31] Y. Mack and M. Rosenblatt, “Multivariate k-nearest neighbor density estimates,” *Journal of Multivariate Analysis*, vol. 9, no. 1, pp. 1–15, 1979.

[32] A. Liu and A. Moitra, “Tensor completion made practical,” in *Advances in Neural Information Processing Systems*, H. Larochelle, M. Ranzato, R. Hadsell, M. Balcan, and H. Lin, Eds., vol. 33, 2020, pp. 18905–18916.

[33] G. Ballard and T. G. Kolda, *Tensor Decompositions for Data Science*. Cambridge University Press, 2025.

[34] C. R. Harris, K. J. Millman, S. J. van der Walt, R. Gommers, P. Virtanen, D. Cournapeau, E. Wieser, J. Taylor, S. Berg, N. J. Smith, R. Kern, M. Picus, S. Hoyer, M. H. van Kerkwijk, M. Brett, A. Haldane, J. F. del Río, M. Wiebe, P. Peterson, P. Gérard-Marchant, K. Sheppard, T. Reddy, W. Weckesser, H. Abbasi, C. Gohlke, and T. E. Oliphant, “Array programming with NumPy,” *Nature*, vol. 585, no. 7825, pp. 357–362, Sep. 2020. [Online]. Available: <https://doi.org/10.1038/s41586-020-2649-2>

[35] D. M. Dunlavy, N. T. Johnson *et al.*, “pyttb: Python Tensor Toolbox, v1.8.2,” Jan. 2025. [Online]. Available: <https://github.com/sandialabs/pyttb>

[36] O. F. López, D. M. Dunlavy, and R. B. Lehoucq, “Zero-truncated Poisson regression for sparse multiway count data corrupted by false zeros,” *Information and Inference: A Journal of the IMA*, vol. 12, no. 3, pp. 1573–1611, 2023.